Journal of Applied Analysis and Computation
Volume 11, Number 3, June 2021, 1371–1390
Website:http://www.jaac-online.com
DOI:10.11948/20200182

TURING INSTABILITY AND PATTERNS OF THE FITZHUGH-NAGUMO MODEL IN SQUARE DOMAIN

Mingzhu Qu[1] and Chunrui Zhang[1,†]

Abstract In this paper, critical conditions of Turing instability for Fitzhugh-Nagumo (FHN) model with diffusion under Neumann boundary conditions are derived. Moreover, different from previous works about the FHN model, we obtain simple bifurcation, double bifurcation, and four-fold bifurcation with stripe pattern, rectangular pattern, spot pattern, square pattern, and highly developed square pattern, respectively. Meanwhile, the theoretical results are applied to two coupled FHN model with diffusion, and the process of the coupling strengths affecting the stability of the model is presented by numerical simulations.

Keywords Turing instability, coupled Fitzhugh-Nagumo, diffusion, pattern.

MSC(2010) 35B32, 35B36, 35K57.

1. Introduction

Pattern dynamics is an important part of nonlinear science. The purpose of the research is to explore the basic law of pattern formation which coexists among various systems. Riley-Benard system, reaction-diffusion system, oscillatory sand table system, and nonlinear optical system in a fluid are the main research objects of pattern dynamics theory and experiment. Reaction-diffusion models are commonly used as mechanisms for pattern formation [16]. Analogous models are used in modeling neural pattern formation [5]. These depend on lateral inhibition and so-called Turing instability. The Turing instability can be defined as a mechanism by which spatially inhomogeneous perturbations of a steady-state grow exponentially, while constant perturbations decay. Bifurcation theory can be used to prove the existence of small-amplitude spatial patterns for these systems [6]. Murray [16] commented that in two-dimensional spatial domains, stripes were difficult to obtain for reaction-diffusion models whereas they arose quite naturally in many neural models. Ermentrout [4] demonstrated a selection mechanism for 'stripe' versus 'spots' in systems of reaction-diffusion and other Turing instability-driven systems. He noted that in linearized equation $e\,(rcosx + scosy)$, where e is the eigenvector, r and s are arbitrary scalars, if $r = 0$ and $s \neq 0$, a 'strip' would occur while if both $r \neq 0$ and $s \neq 0$, a 'spot' would appear.

Pattern is the result of systematic dynamic bifurcation and some space-time symmetry breaking. Generally speaking, the static pattern with periodic distri-

†The corresponding author. Email: math@nefu.edu.cn(C. Zhang)
[1]Department of Mathematics, Northeast Forestry University, Harbin 150040, China

bution in space is caused by Turing instability, while the dynamic pattern with periodic variation with time is caused by Hopf instability or wave instability. Turing patterns mainly include hexagons, quadrilaterals and stripes. In the reaction diffusion system, since the amplitude equation does not exist $A \longrightarrow -A$ reverse symmetry near the critical point and the second-order term of the equation is not zero, the quadrilateral pattern is relatively unstable and difficult to obtain, which has become a difficult point in research. Currently, researchers have derived square and many kinds of super-quadrangle patterns in different experimental systems. Gal et al. [14] used glass with a poor thermal conductivity as the boundary in the Rayleigh-Benard convection system to obtain a stable square pattern. Wagner et al. [31] gained the positive quadrangle pattern in the Faraday experiment by using the external driving frequency, and observed the transformation from the quadrilateral to the hexagonal. Moreover, Li et al. [15] obtained a stable square pattern formed spontaneously under Turing instability by using the double-layer coupled Lengyel-Epstein model.

Turing [29] proposed the pattern dynamics in the study of the reaction-diffusion system in 1952. He used the reaction-diffusion model to explain the patterns displayed on the surface of some organisms, such as the production mechanism of the pattern on the zebra. Turing's mechanism is a kind of instability caused by diffusion. In [29], Turing pointed out that in the reaction-diffusion system, under certain conditions, the stable and homogeneous state could be unstable, and the spatial fixed pattern was generated spontaneously. This process and the resulting pattern were the Turing instability and Turing pattern, the reason for this phenomenon was the instability caused by the different diffusion rates of the two reactants [18, 20, 21, 23, 25–27, 30]. Therefore, it is necessary to study the diffusion dynamics of the Fitzhugh-Nagumo model and the resulting Turing instability.

In 1952, to study the essence of the electrical activity process of the biological nervous system, Hodgkin and Huxley [11] took squid as the experimental object, carried out many experiments by using voltage-clamp technique, and obtained a large number of experimental data about the electrophysiological activity of squid axons. Based on these data, a Hodgkin-Huxley model which can accurately describe the electrical activity of the cell membrane was deduced as follows:

$$\begin{cases} c\dot{V}(t) = -g_{Na}mh(V - V_{Na}) - g_K n^4 (V - V_K) \\ \qquad\qquad - g_L (V - V_L) + I, \\ \dot{m}(t) = \dfrac{m_\infty (V) - m}{\tau_m (V)}, \\ \dot{h}(t) = \dfrac{h_\infty (V) - h}{\tau_h (V)}, \\ \dot{n}(t) = \dfrac{n_\infty (V) - n}{\tau_n (V)}, \end{cases} \tag{H - H}$$

where V is the membrane voltage, g_{Na}, g_K, g_L represent the maximum capacitance of Na^+ ion channel, K^+ ion channel, Cl^+ ion channel, V_{Na}, V_K, V_L represent the equilibrium potential of Na^+, K^+, Cl^+ and other leaking ions, h represents the preparation of sodium ion current, n and m are activation variables, t represents time.

Since the H-H model is a nonlinear differential equation with four variables, although some dynamic behaviors of the system can be obtained by numerical sim-

ulation, it is almost impossible to obtain its analytical solution because of the complexity of the system, so it is hard to study the characteristics and dynamic behavior of the system more deeply from the mathematical point of view. Therefore, some researchers hope to use a simple mathematical model to reflect the complex electrophysiological process of the nervous system. In 1962, Fitzhugh and Nagumo [7,19] simplified the H-H model, and obtained the following two-dimensional Fitzhugh-Nagumo (FHN) model:

$$\begin{cases} \varepsilon \dot{u} = af(u) - v, \\ \dot{v} = u - \delta v, \end{cases} \tag{FHN}$$

where $\varepsilon > 0$, δ are small parameters, $f(u) = u - u^3$, and u represents the membrane potential, v represents the recovery variable, namely, u, v represent the neural neurons.

FHN model is a simple two-dimensional model, which can not only simulate the action potential of neuron electrical activity but also the frequency of neuron discharge. Therefore, it has been studied widely. Many researchers have found that by selecting appropriate parameter values, the system can appear a variety of bifurcation, limit cycle, periodic motion and chaos, and other rich dynamic behavior [1,3,9,10,17,22,24].

In this paper, we add the diffusion to the FHN model and obtain the reaction-diffusion system as follows:

$$\begin{cases} \varepsilon \dfrac{\partial u}{\partial t} = d_1 \Delta u + af(u) - v, \\ \dfrac{\partial v}{\partial t} = d_2 \Delta v + u - \delta v, \end{cases} \tag{1.1}$$

with Neumann boundary conditions

$$\begin{cases} u(x, y, 0) = u_0, v(x, y, 0) = v_0, (x, y) \in \Omega, \\ \dfrac{\partial u}{\partial n} = \dfrac{\partial v}{\partial n} = 0, (x, y) \in \partial\Omega, \end{cases}$$

where $\Omega = [0, l] \times [0, l]$, l is a positive bounded constant which gives out the size of the system in the directions of x and y, n is the outward unit normal vector of the boundary $\partial\Omega$.

As a matter of fact, many researchers also concentrate on the coupled FHN model [2,8,13,28,32]. The interactional neuron model considered by Jalnine [13] consisted of a pair of coupled FHN systems, with the parameters being periodically modulated in antiphase, so that the neurons underwent alternate excitation with a successive transmission of the phase of oscillations from one neuron to another. Song and Xu [28] investigated the delay-coupled FHN system. They found conditional stability, absolute stability, and stability switches of the steady state provoked by the coupling time delay. Moreover, in [32], the authors analyzed the dynamics of the FHN slow-fast system with diffusion and coupling. In the case of two coupled FHN reaction-diffusion, the Turing-Hopf-Turing bifurcation occurred, and they also found the case about the spatial resonance of Turing-Turing bifurcation arising, and two kinds spatially steady-state solutions are found which are synchronous or anti-phased. If considering the coupling between the FHN model with the diffusion,

then we have

$$\begin{cases} \varepsilon \dfrac{\partial u_1}{\partial t} = d_1 \Delta u_1 + af(u_1) - v_1 - \alpha(u_2 - u_1), \\ \dfrac{\partial v_1}{\partial t} = d_2 \Delta v_1 + u_1 - \delta v_1 - \beta(v_2 - v_1), \\ \varepsilon \dfrac{\partial u_2}{\partial t} = d_1 \Delta u_2 + af(u_2) - v_2 + \alpha(u_2 - u_1), \\ \dfrac{\partial v_2}{\partial t} = d_2 \Delta v_2 + u_2 - \delta v_2 + \beta(v_2 - v_1). \end{cases} \tag{1.2}$$

This model is a neuron-coupled system, and it describes layers that are identical in their underlying chemical and physical properties, where α and β measure the coupling strengths, $\alpha > 0$ and $\beta > 0$, which represent the interactions between neurons.

The purpose of this paper is to analyze the stability of the FHN model with diffusion term and the coupled FHN model over a square domain and to discuss the properties of the patterns that they produced. Firstly, in section 2, we give the conditions for the Turing instability of a single FHN model with diffusion in Theorem 2.1. At the same time, we investigate the types of state bifurcation when m and n are in different cases. We obtain spot pattern, square pattern, and highly developed square pattern when the state bifurcation is simple, double, and four-fold respectively. Then, we consider the two coupled FHN model with diffusion in section 3. We obtain the Theorem 3.1 by analyzing the Turing instability and Turing bifurcation of the coupled FHN model. In addition, when the coupling strengths are selected with appropriate values, we can verify the stability of the coupled FHN model from the patterns produced by simulating. Some numerical simulations support our theoretical results in sections 2 and 3, respectively.

2. The FHN model on square domain

2.1. Stability analysis of FHN model

In this section, based on the method of [12], we investigate the Turing bifurcation and Turing instability of the FHN model (1.1) with the diffusion term. Let $\sigma = d_2/d_1$, the system (1.1) can be rewritten into

$$\begin{cases} \dfrac{\partial u}{\partial t} = \dfrac{1}{\varepsilon} d_1 \Delta u + \dfrac{a}{\varepsilon}\left(u - u^3\right) - \dfrac{1}{\varepsilon} v, \\ \dfrac{\partial v}{\partial t} = \sigma d_1 \Delta v + u - \delta v. \end{cases} \quad \text{in} \quad \Omega = [0, l] \times [0, l]. \tag{2.1}$$

The system (2.1) has a unique constant positive steady-state solution $E_1^* = (u_*, v_*)$ under the premise of $a\delta > 1$, where

$$(u_*, v_*) = \left(\sqrt{1 - 1/a\delta}, \sqrt{(a\delta - 1)/a\delta^3}\right), (a\delta > 1).$$

In order to simplify the discussion and the numerical calculation, we transform the homogeneous steady-state solution (u_*, v_*) into $(0, 0)$ by $(u, v) = (\tilde{u} + u_*, \tilde{v} + v_*)$.

Moreover, we transform square domain $\Omega = [0,l] \times [0,l]$ to unit domain $\tilde{\Omega} = [0,1] \times [0,1]$ by transforming $x = l\tilde{x}$ and $y = l\tilde{y}$, then the system (2.1) becomes

$$\begin{cases} \dfrac{\partial \tilde{u}}{\partial t} = \dfrac{1}{\varepsilon} d_1 \dfrac{1}{l^2} \Delta u + \left(\dfrac{a}{\varepsilon} - \dfrac{3a}{\varepsilon} u_*^2 \right) \tilde{u} - \dfrac{1}{\varepsilon} \tilde{v} \\ \qquad\qquad + \left(\dfrac{a}{\varepsilon} u_* - \dfrac{a}{\varepsilon} u_*^3 - \dfrac{1}{\varepsilon} v_* - \dfrac{3a}{\varepsilon} u_*^2 \tilde{u}^2 - \dfrac{a}{\varepsilon} \tilde{u}^3 \right), \\ \dfrac{\partial \tilde{v}}{\partial t} = \sigma d_1 \dfrac{1}{l^2} \Delta v + \tilde{u} - \delta \tilde{v} + (u_* - \delta v_*), \end{cases} \tag{2.2}$$

with

$$\begin{cases} u(\tilde{x}, \tilde{y}, 0) = u_0, v(\tilde{x}, \tilde{y}, 0) = v_0, (\tilde{x}, \tilde{y}) \in \tilde{\Omega}, \\ \dfrac{\partial \tilde{u}}{\partial n} = \dfrac{\partial \tilde{v}}{\partial n} = 0, (\tilde{x}, \tilde{y}) \in \partial \tilde{\Omega}. \end{cases}$$

For the sake of simplify and calculation, we express the d_1, $\tilde{x}$, $\tilde{y}$ and $\tilde{u}$, $\tilde{v}$ as d, x, y and u, v.

Recall that $\mu_k = \left(m^2 + n^2\right)\pi^2$ with $m, n \in \mathbb{N}_0$ is the eigenvalue of $-\Delta$ in two dimensional spatial domain $\tilde{\Omega} = [0,1] \times [0,1]$, where $\mathbb{N}_0$ is a nonnegative integer set, then we can analyze the roots of the following series of equations to get the eigenvalues of the linearized operator.

$$M_{m,n}(\lambda, \sigma) := \begin{pmatrix} -\dfrac{d}{\varepsilon l^2}\left(m^2 + n^2\right)\pi^2 + \dfrac{a}{\varepsilon} - \dfrac{3a}{\varepsilon} u_*^2 - \lambda & -\dfrac{1}{\varepsilon} \\ 1 & -\sigma \dfrac{d}{l^2}\left(m^2 + n^2\right)\pi^2 - \delta - \lambda \end{pmatrix},$$

$m, n \in \mathbb{N}_0$.

The characteristic equations of $M_{m,n}$ for some m, n are the following sequence of quadratic equations:

$$\Lambda_{m,n}(\lambda, \sigma) = \det M_{m,n}(\lambda, \sigma) := \lambda^2 - \operatorname{trace}(m,n)\lambda + \det(m,n) = 0, m, n \in \mathbb{N}_0, \tag{2.3}$$

with

$$\begin{aligned} \operatorname{trace}(m,n) &= -\left(\frac{1}{\varepsilon} + \sigma\right) \frac{d\left(m^2 + n^2\right)\pi^2}{l^2} + \frac{a}{\varepsilon} - \frac{3au_*^2}{\varepsilon} - \delta, \\ \det(m,n) &= \frac{\sigma}{l^4 \varepsilon} d^2 \left(m^2 + n^2\right)^4 \pi^4 + \left(3a\sigma u_*^2 + \delta - a\sigma\right) \frac{d\left(m^2 + n^2\right)\pi^2}{l^2 \varepsilon} \\ &\quad + \left(\frac{3a\delta u_*^2}{\varepsilon} + \frac{1}{\varepsilon} - \frac{a\delta}{\varepsilon} \right). \end{aligned}$$

In the following part, we rewrite $k^2 = m^2 + n^2$ for convenience, where $m, n \in \mathbb{N}_0$ and $k \in \mathbb{N}_0$. With the aim to resolve the stabilization problem of system (2.2), several hypotheses are presented.

(H_0) $\quad 0 < \dfrac{1}{3} - \dfrac{1}{3a\delta} < u_*^2 < \dfrac{1}{3} - \dfrac{\varepsilon\delta}{3a}, a < 0, \delta < 0.$

Under the hypothesis (H_0), when $k = 0$, all eigenvalues of $\Lambda_0(\lambda, \sigma)$ have negative real parts, and $\operatorname{trace}(k) < 0$, for $k \in \mathbb{N}_0$. In the following, we discuss the

conditions under which Turing instability occurs with $k \in \mathbb{N}, k \neq 0$.

(H_1) $0 < \sigma < \sigma_1$, where

$$\sigma_1 \triangleq \frac{a\delta\varepsilon\left(1-3u_*^2\right)}{a^2\varepsilon + 9a^2\varepsilon u_*^4 + 4a\delta - 6au_*^2(a\varepsilon+2\delta) - 4} + 2\sqrt{\frac{\delta^2\varepsilon\left(-a\delta+3a\delta u_*^2+1\right)}{\left(a^2\varepsilon + 9a^2\varepsilon u_*^4 + 4a\delta - 6au_*^2(a\varepsilon+2\delta) - 4\right)^2}}.$$

(H_2) $0 < \sigma < \sigma_2(d), \sigma_2(d) \triangleq \dfrac{-l^2\delta}{d\pi^2 + 3au_*^2l^2 - al^2}$.

Let $k_{\min}^2$ be the minimal point of function $\det(k)$ on $k^2 \in \mathbb{R}_+$, then

$$k_{\min} = \sqrt{\frac{l^2}{2d}\frac{-\delta - 3a\sigma u_*^2 + a\sigma}{\sigma\pi^2}}.$$

By hypothesis (H_1), we can get $\min\limits_{k\in\mathbb{R}_+} \det(k) < 0$ and $3a\sigma u_*^2 + \delta - a\sigma < 0$. Moreover, hypothesis (H_2) guarantees that the minimal point

$$k_{\min} > \sqrt{\frac{1}{2}}.$$

It ought to be seen that $\sigma = \sigma_2(d)$ decreases monotonically with respect to d and intersects with $\sigma = \sigma_1$ at the point $d = d_0$. Let $\sigma_A(d) = \min\limits_{d>0}\{\sigma_1, \sigma_2(d)\}$, then

$$\sigma_A(d) = \begin{cases} \sigma_1, 0 < d \leq d_0, \\ \sigma_2(d), d \geq d_0. \end{cases} \tag{2.4}$$

To deduce main results, two lemmas are given, which will be used in main results.

Lemma 2.1. *Assume that* (H_0) *holds, then hypotheses* (H_1) *and* (H_2) *hold if and only if* $0 < \sigma < \sigma_A(d)$, $d > 0$.

Denote

$$\sigma_*(k,d) = \frac{\left(a\delta l^2 - 3a\delta u_*^2 l^2 - l^2 - \delta dk^2\pi^2\right)l^2}{dk^2\pi^2\left(dk^2\pi^2 + 3au_*^2l^2 - al^2\right)}, \quad \text{for} \quad d > d_k, \tag{2.5}$$

where $d_k = \dfrac{\left(a\delta - 3a\delta u_*^2 - 1\right)l^2}{\delta k^2\pi^2}$, then $\det(k) = 0$ when $\sigma = \sigma_*(k,d)$.

Let $d_M(k)$ be the point at which the monotonicity of the function changes, that is function $\sigma = \sigma_*(k,d)$ increases monotonically if $d_k < d < d_M(k)$, and $\sigma = \sigma_*(k,d)$ decreases monotonically if $d_M(k) < d < +\infty$. Therefore, $\sigma = \sigma_*(k,d)$ can take the maximum value σ_1 at $d_M(k)$.

Lemma 2.2. *Assume that* (H_0) *holds, function* $\sigma = \sigma_*(k,d)$ *has the following properties.*

(i) As for $k_i < k_{i+1}$, $k_i \in \mathbb{N}, i = 1, 2, 3\cdots$, *there is only one root* $d_{k_1,k_2} \in (d_M(k_2), d_M(k_1))$ *meets* $\sigma_*(k_1,d) = \sigma_*(k_2,d)$ *for* $d > 0$. *Moreover,*

$$\sigma_*(k_1,d) > \sigma_*(k_2,d) > \sigma_*(k_3,d) > \cdots, \text{for } d > d_{k_i,k_{i+1}}.$$

(ii) Denote $d_{k_0,k_1} = +\infty$, *and*

$$\sigma_* \triangleq \sigma_* (d) = \sigma_* (k, d), d \in \left(d_{k_i,k_{i+1}}, d_{k_{i-1},k_i}\right), k_i \in \mathbb{N}, i = 1, 2, 3 \cdots .$$

Then

$$\sigma_* (d) \leq \sigma_A (d), 0 < d < +\infty.$$

Furthermore, $\sigma_* (d) = \sigma_A (d)$ *if and only if* $d = d_M (k)$, $k \in \mathbb{N}$.

The relation of $\sigma = \sigma_1$, $\sigma = \sigma_2 (d)$ and $\sigma = \sigma_* (k, d)$ is presented in Fig.1, where $d > 0$, $k = 5, 10, 13 \cdots$. Meanwhile, the critical curve of Turing instability is shown in Fig.2.

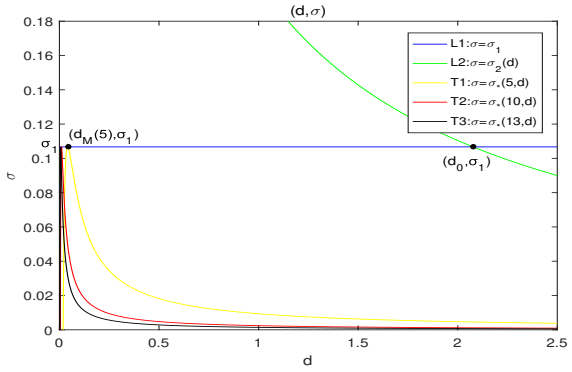

Figure 1. The figure of functions $\sigma = \sigma_1$, $\sigma = \sigma_2 (d)$ and $\sigma = \sigma_* (k, d)$, $d > 0$, $k = 5, 10, 13 \cdots$, in (d, σ) plane.

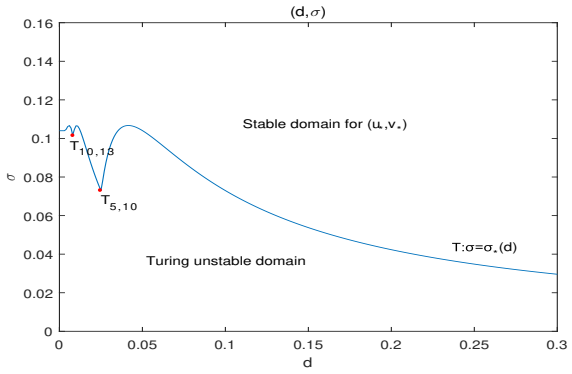

Figure 2. The Turing bifurcation line T : $\sigma = \sigma_* (d)$, $d > 0$.

As a consequence, in the light of the above analysis, a theorem is presented in the following to derive the conditions for Turing bifurcation and Turing instability of system (1.1).

Theorem 2.1. *Assume that* (H_0) *holds.*

(1) For any given $k_1 \in \mathbb{N}$, *when* $\sigma = \sigma_* (k_1, d)$, *the system (1.1) occurs* $k_1 -$*mode Turing bifurcation at* (u_*, v_*).

(2) $\sigma = \sigma_*(d)$, $d > 0$ *is the critical curve of Turing instability.*

(i) If $\sigma > \sigma_*(d)$, $d > 0$, *the system (1.1) is asymptotically stable at positive equilibrium* (u_*, v_*).

(ii) If $0 < \sigma < \sigma_*(d)$, $d > 0$, *Turing instability occurs in the system (1.1) at positive equilibrium* (u_*, v_*).

Proof. When $\sigma = \sigma_*(k_1, d)$, we can get $\det(k_1) = 0$. The characteristic equation (2.3) becomes

$$\Lambda_{k_1}(\lambda, \sigma) := \lambda^2 - \operatorname{trace}(k_1)\lambda = 0. \tag{2.6}$$

The Eq.(2.6) has a zero root, and the other root of $\Lambda_{k_1}(\lambda, \sigma)$ has negative real part. That is, the system (1.1) occurs Turing bifurcation at (u_*, v_*) when $\sigma = \sigma_*(k_1, d)$.

If $\sigma > \sigma_*(d)$, $d > 0$, then $\det(k_1) > 0$. (H_0) guarantees $\operatorname{trace}(k_1) < 0$, so all roots of $\Lambda_{k_1}(\lambda, \sigma)$ have negative real parts. On the other hand, if $0 < \sigma < \sigma_*(d)$, $d > 0$, $\det(k_1) < 0$, then the system (1.1) is Turing instability. □

Remark 2.1. $\mu_k = k^2\pi^2$ is the eigenvalue of $-\Delta$, where k is a nonnegative integer satisfies $k^2 = m^2 + n^2, m, n \in \mathbb{N}_0$. Then one, two, or more pairs (m, n) may exist such that the eigenvalues will have single, double or higher multiplicity respectively. Hence, the state bifurcation will be simple, double, three-fold, four-fold and so on.

2.2. Numerical simulation of the FHN model with diffusion

According to the above analysis, we select the parameters a, δ, ε and l as $a = -2.25, \delta = -0.6, \varepsilon = 0.1067, l = 2$.

We obtain $(u_*, v_*) = (0.5092, 0.8486)$ which satisfies the hypothesis (H_0). Through (H_1), (H_2), (2.4) and (2.5), we can get $\sigma_1 = 0.1067$,

$$\sigma_A(d) = \begin{cases} 0.1067, 0 < d \le 2.0786, \\ \dfrac{2.4}{d\pi^2 + 1.9993}, d \ge 2.0786, \end{cases}$$

and

$$\sigma_*(k_1, d) = \frac{-11.2016 + 2.4dk_1^2\pi^2}{dk_1^2\pi^2\left(dk_1^2\pi^2 + 1.9993\right)}.$$

By setting $k_1 = 10$, we obtain $d_{10,13} = 0.0082$ and $d_{5,10} = 0.0252$. Choose $d = d_1 = 0.01 \in [d_{10,13}, d_{5,10}]$, thus $\sigma_* = \sigma_*(10, 0.01) = 0.1066$. Therefore, system (1.1) with $d = 0.01$ undergoes 10-mode Turing bifurcation near equilibrium $(0.5092, 0.8486)$ at $\sigma = 0.1066$. We define the patterns in square domain $\Omega = [0, 2] \times [0, 2]$. Since $k_1^2 = m^2 + n^2$, $k \in \mathbb{N}$, the selection of m and n have several cases. In the following, we list the corresponding state bifurcation in Table 1.

Through Table 1, the types of bifurcation are divided into three types. As a result, we give the numerical simulations which are divided into three cases:

Case I Simple bifurcation with 'stripe' and 'rectangular' patterns are presented in Figs.3 and 4.

Table 1. Five types patterns when $k_1^2 = 100 = m_i^2 + n_i^2, i = 1, 2, 3, 4$.

Type of bifurcation	$k_1^2 = 100 = m_i^2 + n_i^2, i = 1, 2, 3, 4$	Pattern
simple	$m_1 = 10, n_1 = 0$	stripe
simple	$m_3 = 8, n_3 = 6$	rectangular
double	interaction of $m_1 = 0, n_1 = 10$ and $m_2 = 0, n_2 = 10$	spot
double	interaction of $m_3 = 8, n_3 = 6$ and $m_4 = 6, n_4 = 8$	square
four-fold	interaction of $m_1 = 10, n_1 = 0, m_2 = 0, n_2 = 10$, $m_3 = 8, n_3 = 6$ and $m_4 = 6, n_4 = 8$	highly developed square

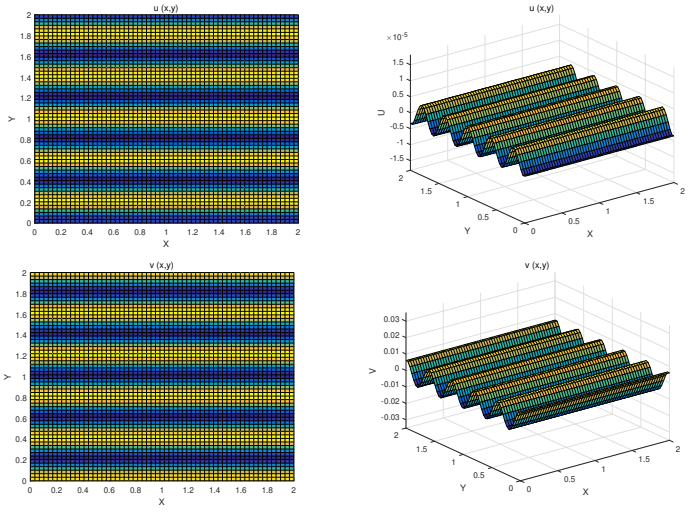

Figure 3. Stripe patterns when $k_1 = 10$, $m_1 = 10$, $n_1 = 0$. The initial values are $u0 = 0.00000002\cos(5\pi x)$, $v0 = 0.007\cos(5\pi y)$.

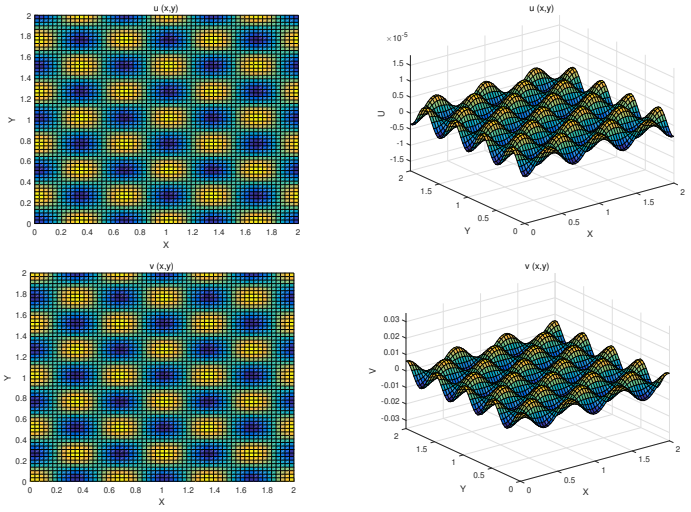

Figure 4. Rectangular patterns when $k_1 = 10$, $m_3 = 8$, $n_3 = 6$. The initial values are $u0 = 0.00000002\cos(4\pi x)\cos(3\pi y)$, $v0 = 0.007\cos(3\pi x)\cos(4\pi y)$.

Case II Double bifurcation with 'spot' and 'square' patterns are presented in Figs.5 and 6.

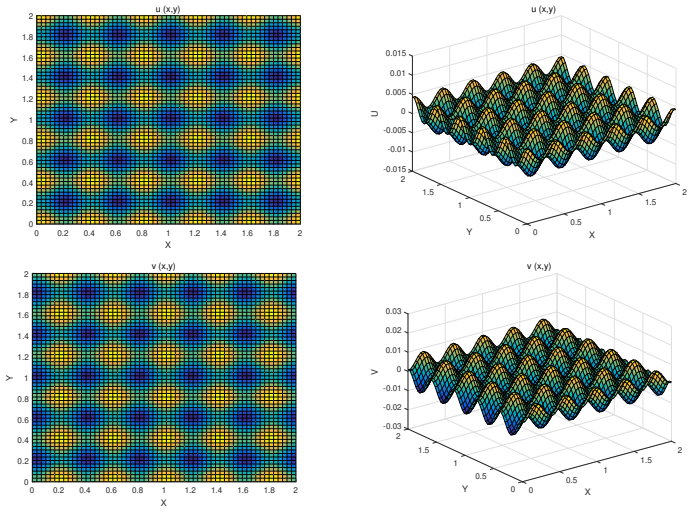

Figure 5. Spot patterns when $k_1 = 10$, $m_1 = 10$, $n_1 = 0$, $m_2 = 0$, $n_2 = 10$ by interacting $m_{1,2}$, $n_{1,2}$ two modes. The initial values are $u0 = 0.002\cos(5\pi x) + 0.003\cos(5\pi y)$, $v0 = 0.005\cos(5\pi y) - 0.004\cos(5\pi x)$.

Case III Four-fold bifurcation with highly developed square patterns are presented in Fig.7.

3. The coupled FHN model on square domain

3.1. Dynamic properties of coupled FHN model

In this section, we consider the coupled FHN model. Let $\sigma = d_2/d_1$, and recall $d = d_1$ for convenience, then the system (1.2) can be rewritten as

$$\begin{cases} \dfrac{\partial u_1}{\partial t} = \dfrac{d}{\varepsilon}\Delta u_1 + \dfrac{a}{\varepsilon} f(u_1) - \dfrac{1}{\varepsilon} v_1 - \dfrac{\alpha}{\varepsilon}(u_2 - u_1), \\ \dfrac{\partial v_1}{\partial t} = \sigma d\Delta v_1 + u_1 - \delta v_1 - \beta(v_2 - v_1), \\ \dfrac{\partial u_2}{\partial t} = \dfrac{d}{\varepsilon}\Delta u_2 + \dfrac{a}{\varepsilon} f(u_2) - \dfrac{1}{\varepsilon} v_2 + \dfrac{\alpha}{\varepsilon}(u_2 - u_1), \\ \dfrac{\partial v_2}{\partial t} = \sigma d\Delta v_2 + u_2 - \delta v_2 + \beta(v_2 - v_1), \end{cases} \tag{3.1}$$

with

$$\begin{cases} u_1(x, y, 0) = u_0, v_1(x, y, 0) = v_0, u_2(x, y, 0) = u_0, v_2(x, y, 0) = v_0, (x, y) \in \Omega, \\ \dfrac{\partial u_1}{\partial n} = \dfrac{\partial v_1}{\partial n} = \dfrac{\partial u_2}{\partial n} = \dfrac{\partial v_2}{\partial n} = 0, (x, y) \in \partial\Omega. \end{cases}$$

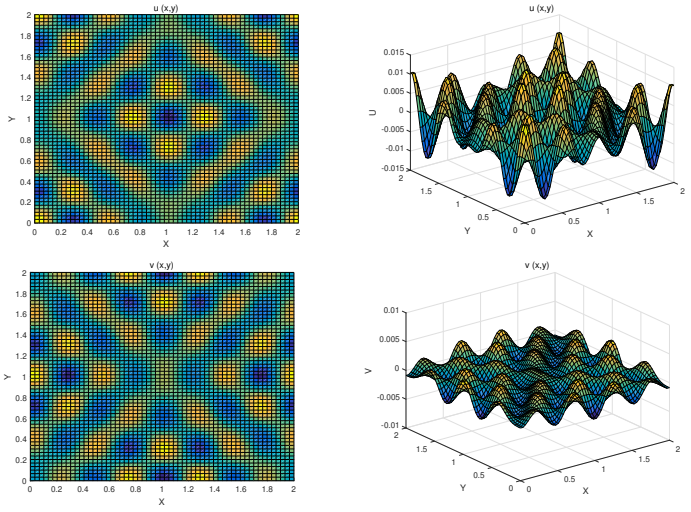

Figure 6. Square patterns when $k_1 = 10$, $m_3 = 8$, $n_3 = 6$, $m_4 = 6$, $n_4 = 8$ by interacting $m_{3,4}$, $n_{3,4}$ two modes. The initial values are $u0 = 0.007\cos(4\pi x)\cos(3\pi y) + 0.005\cos(3\pi x)\cos(4\pi y)$, $v0 = 0.001\cos(3\pi x)\cos(4\pi y) - 0.002\cos(4\pi x)\cos(3\pi y)$.

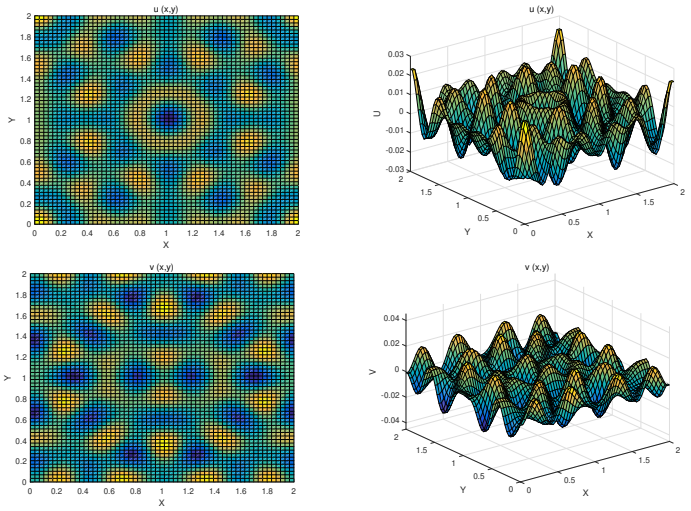

Figure 7. Highly developed square patterns when $k_1 = 10$, $m_1 = 10$, $n_1 = 0$, $m_2 = 0$, $n_2 = 10$, $m_3 = 8$, $n_3 = 6$, $m_4 = 6$, $n_4 = 8$ by interacting $m_{1,2,3,4}$, $n_{1,2,3,4}$ four modes. The initial values are $u0 = 0.007\cos(5\pi x) + 0.005\cos(5\pi y) + 0.006\cos(4\pi x)\cos(3\pi y) + 0.009\cos(3\pi x)\cos(4\pi y)$, $v0 = 0.007\cos(5\pi y) - 0.005\cos(5\pi x) + 0.006\cos(3\pi x)\cos(4\pi y) - 0.009\cos(4\pi x)\cos(3\pi y)$.

We investigate the stability of the steady state $E_2^* = (u_*, v_*, u_*, v_*)$, here $u_* = \sqrt{1 - 1/a\delta}$ and $v_* = \sqrt{(a\delta - 1)/a\delta^3}$. For simplification, we shift the positive equilibrium to the origin by transformation, and transform the square domain into the unit domain, then we obtain

$$\begin{cases} \dfrac{\partial u_1}{\partial t} = \dfrac{d}{\varepsilon l^2}\Delta u_1 + f_1(u_1, v_1, u_2, v_2), \\ \dfrac{\partial v_1}{\partial t} = \sigma d\Delta v_1 + g_1(u_1, v_1, u_2, v_2), \\ \dfrac{\partial u_2}{\partial t} = \dfrac{d}{\varepsilon l^2}\Delta u_2 + f_2(u_1, v_1, u_2, v_2), \\ \dfrac{\partial v_2}{\partial t} = \sigma d\Delta v_2 + g_2(u_1, v_1, u_2, v_2), \end{cases} \tag{3.2}$$

where

$$f_1 = \left(\frac{a}{\varepsilon} + \frac{\alpha}{\varepsilon} - \frac{3a}{\varepsilon}u_*^2\right)u_1 - \frac{1}{\varepsilon}v_1 - \frac{\alpha}{\varepsilon}u_2 + \frac{a}{\varepsilon}u_* - \frac{a}{\varepsilon}u_*^3 - \frac{1}{\varepsilon}v_* - \frac{3a}{\varepsilon}u_*u_1^2 - \frac{a}{\varepsilon}u_1^3,$$
$$g_1 = u_1 + (\beta - \delta)v_1 - \beta v_2 + u_* - \delta v_*,$$
$$f_2 = -\frac{\alpha}{\varepsilon}u_1 + \left(\frac{a}{\varepsilon} + \frac{\alpha}{\varepsilon} - \frac{3a}{\varepsilon}u_*^2\right)u_2 - \frac{1}{\varepsilon}v_2 - \frac{1}{\varepsilon}v_* + \frac{a}{\varepsilon}u_* - \frac{a}{\varepsilon}u_*^3 - \frac{3a}{\varepsilon}u_*u_2^2 - \frac{a}{\varepsilon}u_2^3,$$
$$g_2 = -\beta v_1 + u_2 + (\beta - \delta)v_2 + u_* - \delta v_*.$$

The characteristic equations for E_2^* are the following sequence of quadratic equations.

$$\Delta(k)(\lambda) = \begin{vmatrix} \frac{a}{\varepsilon} - \frac{dk^2\pi^2}{l^2\varepsilon} + \frac{\alpha}{\varepsilon} - \lambda - \frac{3au_*^2}{\varepsilon} & -\frac{1}{\varepsilon} & -\frac{\alpha}{\varepsilon} & 0 \\ 1 & \beta - \delta - \frac{k^2\pi^2\theta d}{l^2} - \lambda & 0 & -\beta \\ -\frac{\alpha}{\varepsilon} & 0 & \frac{a}{\varepsilon} - \frac{dk^2\pi^2}{l^2\varepsilon} + \frac{\alpha}{\varepsilon} - \lambda - \frac{3au_*^2}{\varepsilon} & -\frac{1}{\varepsilon} \\ 0 & -\beta & 1 & \beta - \delta - \frac{k^2\pi^2\theta d}{l^2} - \lambda \end{vmatrix}$$

which can be written as

$$\Delta(k)(\lambda) = \Gamma_1(k)(\lambda)\Gamma_2(k)(\lambda) = 0, k \in N_0, \tag{3.3}$$

where

$$\Gamma_1(k)(\lambda) = \lambda^2 - T_1(k)\lambda + D_1(k) = 0,$$
$$\Gamma_2(k)(\lambda) = \lambda^2 - T_2(k)\lambda + D_2(k) = 0,$$

and

$$T_1(k) = -\left(\frac{1}{\varepsilon} + \sigma\right)\frac{dk^2\pi^2}{l^2} + \frac{a}{\varepsilon} - \frac{3au_*^2}{\varepsilon} - \delta,$$
$$D_1(k) = \frac{\sigma}{\varepsilon}\frac{d^2k^4\pi^4}{l^4} + \left(\frac{3a\sigma u_*^2}{\varepsilon} + \frac{\delta}{\varepsilon} - \frac{a\sigma}{\varepsilon}\right)\frac{dk^2\pi^2}{l^2} + \frac{1}{\varepsilon} + \frac{3a\delta u_*^2}{\varepsilon} - \frac{a\delta}{\varepsilon},$$
$$T_2(k) = -\left(\frac{1}{\varepsilon} + \sigma\right)\frac{dk^2\pi^2}{l^2} + \frac{a}{\varepsilon} - \frac{3au_*^2}{\varepsilon} - \delta + 2\left(\frac{\alpha}{\varepsilon} + \beta\right),$$
$$D_2(k) = \frac{\sigma}{\varepsilon}\frac{d^2k^4\pi^4}{l^4} + \left(\left(3au_*^2 - 2\alpha - a\right)\frac{\sigma}{\varepsilon} + (\delta - 2\beta)\frac{1}{\varepsilon}\right)\frac{dk^2\pi^2}{l^2} + \frac{1}{\varepsilon}$$

$$+\frac{1}{\varepsilon}\left(3au_*^2-2\alpha-a\right)(\delta-2\beta).$$

We suppose that

$(\mathrm{A}_0)\ \dfrac{a}{\varepsilon}-\dfrac{3au_*^2}{\varepsilon}-\delta+2\left(\dfrac{\alpha}{\varepsilon}+\beta\right)<0.$

$(\mathrm{A}_0)'\ 3a\delta u_*^2-a\delta+1>0, 1+\left(3au_*^2-2\alpha-a\right)(\delta-2\beta)>0.$

By assumption (A_0) and $(\mathrm{A}_0)'$, we have $T_1(0)<0$, $D_1(0)>0$, $T_2(0)<0$ and $D_2(0)>0$. Hence, when $k=0$ all eigenvalues of $\Delta(0)(\lambda)$ have negative real parts, and $T_1(k)<T_2(k)<0$, for $k\in\mathbb{N}_0$.

In this section, we mainly consider the effect of coupling strengths on the stability of system (3.2). We can obtain $T_1(k)<0$, $D_1(k)>0$ with (A_0), $(\mathrm{A}_0)'$ and $3a\sigma u_*^2+\delta-a\sigma>0$, then all the roots of $\Gamma_1(k)(\lambda)$ have negative real parts for any given $k\in\mathbb{N}$. We will only need to discuss the roots of $\Gamma_2(k)(\lambda)$ in the following.

Suppose that

$(\mathrm{A}_1)\ 0<\sigma<\sigma_1^{'}, \sigma_1^{'}\triangleq p+2\sqrt{q}$, where

$$p=\frac{\varepsilon(2\beta-\delta)\left(a\left(3u^2-1\right)-2\alpha\right)}{4\left(\alpha^2\varepsilon-4\alpha\beta+2\alpha\delta-1\right)+a^2\varepsilon\left(1-3u^2\right)^2+4a\left(3u^2-1\right)\left(-\alpha\varepsilon+2\beta-\delta\right)},$$

$$q=\frac{\varepsilon(\delta-2\beta)^2\left(4\alpha\beta-2\alpha\delta-a\left(3u^2-1\right)(2\beta-\delta)+1\right)}{\left(4\left(\alpha^2\varepsilon-4\alpha\beta+2\alpha\delta-1\right)+a^2\varepsilon\left(1-3u^2\right)^2+4a\left(3u^2-1\right)\left(-\alpha\varepsilon+2\beta-\delta\right)\right)^2}.$$

$(\mathrm{A}_2)\ 0<\sigma<\sigma_2^{'}(d), \sigma_2^{'}(d)\triangleq\dfrac{-\delta l^2+2\beta l^2}{\pi^2 d+3au_*^2l^2-al^2-2\alpha l^2}.$

We can calculate that $k_{\min}^2$ is the minimum point of the equation $D_2(k)$,

$$k_{\min}=\sqrt{\frac{l^2}{2d}\frac{-\delta+2\beta-3a\theta u_*^2+2\alpha\sigma+a\sigma}{\sigma\pi^2}}, k^2\in\mathbb{R}_+.$$

Assumption (A_1) guarantees $\min\limits_{k\in\mathbb{R}_+}D_2(k)<0$ and $\delta-2\beta+3a\sigma u_*^2-2\alpha\sigma-a\sigma<0$. Moreover, assumption (A_2) guarantees the minimum value point $k_{\min}>\sqrt{1/2}$.

It is obviously that $\sigma=\sigma_2^{'}(d)$ intersects with $\sigma=\sigma_1^{'}$ at the point $d=d_0^{'}$. We take $\sigma_A^{'}(d)=\min\limits_{d>0}\left\{\sigma_1^{'}, \sigma_2^{'}(d)\right\}$, then

$$\sigma_A^{'}(d)=\begin{cases}\sigma_1^{'}, 0<d\le d_0^{'},\\ \sigma_2^{'}(d), d\ge d_0^{'}.\end{cases}$$

Denote

$$\sigma_*^{'}(k,d)=\frac{\left((2\beta-\delta)dk^2\pi^2-l^2-\left(3au_*^2-2\alpha-a\right)(\delta-2\beta)l^2\right)l^2}{dk^2\pi^2\left(dk^2\pi^2+3au_*^2l^2-al^2-2\alpha l^2\right)}, d>d_k^{'}, k\in\mathbb{N},$$

where $d_k^{'}=\dfrac{\left(\left(3au_*^2-2\alpha-a\right)(\delta-2\beta)+1\right)l^2}{(2\beta-\delta)k^2\pi^2}$, then $D_2(k)=0$ when $\sigma=\sigma_*^{'}(k,d)$.

As for $k_i<k_{i+1}$, $k_i\in\mathbb{N}, i=1,2,3\cdots$, there is only one root $d_{k_1,k_2}^{'}\in\left(d_M^{'}(k_2), d_M^{'}(k_1)\right)$ meets $\sigma_*^{'}(k_1,d)=\sigma_*^{'}(k_2,d)$ for $d>0$. Furthermore,

$$\sigma_*^{'}(k_1,d)>\sigma_*^{'}(k_2,d)>\sigma_*^{'}(k_3,d)>\cdots, d>d_{k_i,k_{i+1}}^{'}.$$

Let $d^{'}_{k_0,k_1} = d_{k_0,k_1} = +\infty$, and

$$\sigma_*^{'}(d) = \sigma_*^{'}(k,d), d \in \left(d^{'}_{k_i,k_{i+1}}, d^{'}_{k_{i-1},k_i}\right), k_i \in \mathbb{N}, i = 1,2,3,\cdots.$$

Then

$$\sigma_*^{'}(d) \leq \sigma_A{}^{'}(d), 0 < d < +\infty.$$

The relation of the equations $\sigma = \sigma_1^{'}$, $\sigma = \sigma_2^{'}(d)$ and $\sigma_*^{'}(k,d)$ is presented in Fig.8, where $d > 0$, $k = 5, 10, 13\cdots$. Moreover, the critical curve of Turing instability is presented in Fig.9.

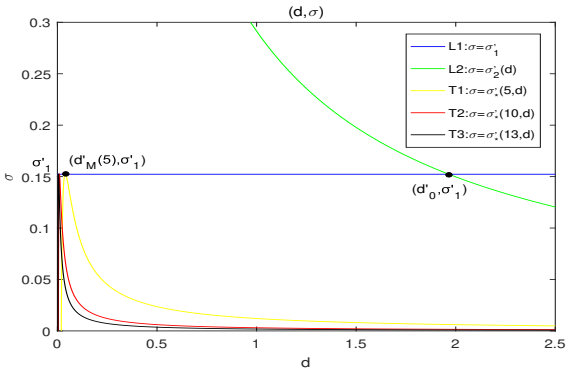

Figure 8. The figure of functions $\sigma = \sigma_1^{'}$, $\sigma = \sigma_2^{'}(d)$ and $\sigma_*^{'}(k,d)$, $d > 0$, $k = 5, 10, 13\cdots$, in (d,σ) plane.

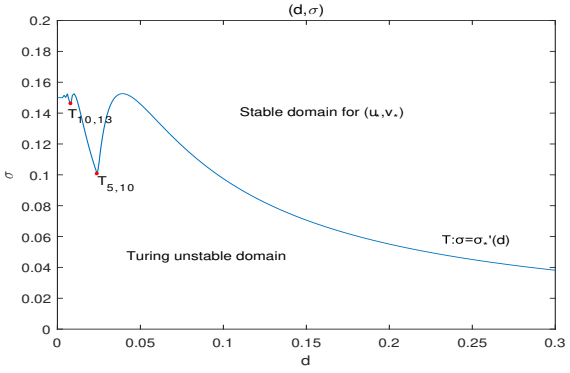

Figure 9. The Turing bifurcation line T : $\sigma = \sigma_*^{'}(d)$, $d > 0$.

Let $\sigma_M(d) = \max\limits_{d>0}\left\{\sigma_*^{'}(d), \sigma_*(d)\right\}$, then we have the following theorem.

Theorem 3.1. *Assume that* (A_0) *and* $(A_0)^{'}$ *hold.*

(1) For any given $k_1 \in \mathbb{N}$. *If* $3a\sigma u_*^2 + \delta - a\sigma > 0$ *hold, the system (1.2) occurs* $k_1 -$ *mode Turing bifurcation at* (u_*, v_*, u_*, v_*) *when* $\sigma = \sigma_*^{'}(k_1, d)$.

(2) $\sigma = \sigma_M(d)$, $d > 0$ *is the critical curve of Turing instability.*

(i) When $\sigma > \sigma_M(d)$, $d > 0$, *the system (1.2) is asymptotically stable at positive equilibrium* (u_*, v_*, u_*, v_*).

(ii) When $0 < \sigma < \sigma_M(d)$, $d > 0$, *Turing instability will happen in the system (1.2) at positive equilibrium* (u_*, v_*, u_*, v_*).

Proof. When $\sigma = \sigma_*^{'}(k_1, d)$, we obtain $D_2(k_1) = 0$. Therefore, the characteristic equation (3.3) becomes

$$\begin{aligned}\Delta(k_1)(\lambda) &= \Gamma_1(k_1)(\lambda)\left(\lambda^2 - T_2(k_1)\lambda\right)\\ &= \left(\lambda^2 - T_1(k_1)\lambda + D_1(k_1)\right)\left(\lambda^2 - T_2(k_1)\lambda\right)\\ &= 0.\end{aligned}$$

By assumption (A_0), we can get $T_2(k_1) < 0$. Hence, $T_1(k_1) < T_2(k_1) < 0$. In addition, $3a\sigma u_*^2 + \delta - a\sigma > 0$ and $(A_0)^{'}$ guarantee $D_1(k_1) > 0$, so the roots of $\Gamma_1(k_1)$ have negative real parts for any $k_1 \in \mathbb{N}$. That is, $\Delta(k_1)(\lambda)$ has a zero root, and all the other roots of $\Delta(k_1)(\lambda)$ have negative real parts.

We have $\sigma > \sigma_*(d)$ and $\sigma > \sigma_*^{'}(d)$ when $\sigma > \sigma_M(d)$. Hence, $D_1(k_1) > 0$ and $D_2(k_1) > 0$. Combining with (A_0), we obtain that all roots of $\Delta(k_1)(\lambda)$ have negative real parts for any $k_1 \in \mathbb{N}$. If $0 < \sigma < \sigma_M(d)$, we have two cases. One is $0 < \sigma < \sigma_*(d)$ with $\sigma_*(d) > \sigma_*^{'}(d)$, then $D_1(k_1) < 0$. The other is $0 < \sigma < \sigma_*^{'}(d)$ with $\sigma_*^{'}(d) > \sigma_*(d)$, then $D_2(k_1) < 0$. However, in either case above, $\Delta(k_1)(\lambda)$ has at least one positive root, the system (1.2) is Turing instability. □

3.2. Numerical simulation of the FHN model with coupling

Let $a = -2.25$, $\delta = -0.6$, $l = 2$, and $\varepsilon = 0.153$, $\alpha = 0.18$, $\beta = 0.08$, so we have $u_* = 0.5092$, $v_* = 0.8486$ and $\sigma_1^{'} = 0.1528$. Furthermore,

$$\sigma_*^{'}(k_1, d) = \frac{3.04dk_1^2\pi^2 - 14.2997}{dk_1^2\pi^2\left(dk_1^2\pi^2 + 0.5593\right)}, k_1 \in \mathbb{N}.$$

By setting $k_1 = 10$, we obtain $d_{10,13}^{'} = 0.0078$, $d_{5,10}^{'} = 0.0243$. Choose $d = d_1 = 0.01 \in \left[d_{10,13}^{'}, d_{5,10}^{'}\right]$, thus $\sigma_*^{'}(10, 0.01) = 0.1526$.

We select $\sigma = 0.14 \in (0.1066, 0.1526)$, then $\sigma > \sigma_*(10, 0.01)$, $D_1(k_1) > 0$, all the roots of $\Gamma_1(k_1)(\lambda)$ have negative real parts. Since $0 < \sigma < \sigma_*^{'}(10, 0.01)$, $D_2(k_1) < 0$, so $\Gamma_2(k_1)(\lambda)$ has at least one positive root. Therefore, the system (1.2) is Turing instability at equilibrium E_2^* when $\sigma = 0.14$.

According to the above analysis, if Turing instability occurs in the system (1.2), then α and β should satisfy the following inequalities:

$$\begin{cases}\dfrac{a}{\varepsilon} - \dfrac{3a{u_{1*}}^2}{\varepsilon} - \delta + 2\left(\dfrac{\alpha}{\varepsilon} + \beta\right) < 0,\\ \dfrac{1}{\varepsilon} + \dfrac{1}{\varepsilon}\left(3a{u_{1*}}^2 - a - 2\alpha\right)(\delta - 2\beta) > 0,\\ \dfrac{\theta}{\varepsilon}\dfrac{d^2k^4\pi^4}{l^4} + \left(\left(3a{u_{1*}}^2 - 2\alpha - a\right)\dfrac{\theta}{\varepsilon} + (\delta - 2\beta)\dfrac{1}{\varepsilon}\right)\dfrac{dk^2\pi^2}{l^2}\\ \quad + \dfrac{1}{\varepsilon} + \dfrac{1}{\varepsilon}\left(3a{u_{1*}}^2 - a - 2\alpha\right)(\delta - 2\beta) < 0.\end{cases} \tag{3.4}$$

Substituting $a = -2.25$, $\delta = -0.6$, $\varepsilon = 0.153$, $l = 2$, $\sigma = 0.14$, $d = 0.01$ into (3.4), we can get (3.5)

$$\begin{cases} 13.1578\alpha + 2\beta - 2.6883 < 0, \\ 26.3156\alpha\beta + 7.8947\alpha - 6.5769\beta + 4.6079 > 0, \\ 26.3156\alpha\beta + 3.3991\alpha - 39.0425\beta + 1.612 < 0. \end{cases} \tag{3.5}$$

We can solve the value range of coupling strengths α and β from inequalities (3.5), and it is shown in Fig.10.

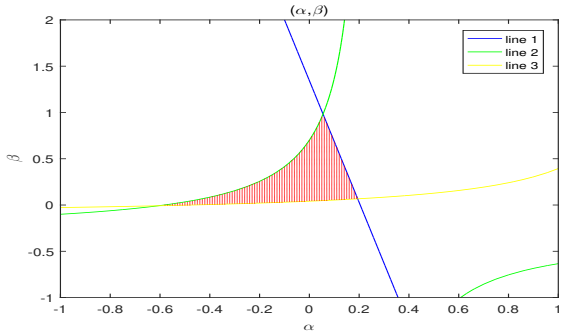

Figure 10. The region of coupling strengths α and β when $d = 0.01$, $\sigma = 0.14$, $a = -2.25$, $\delta = -0.6$, $\varepsilon = 0.153$, $l = 2$.

Remark 3.1. Suppose (A_0) and $(A_0)'$ hold.

(1) Assuming that there is no diffusion term in the system, and we set $\alpha = \beta = 0$, removing the coupling, then the ODE system (1.1) is asymptotically stable at positive equilibrium (u_*, v_*). When the coupling strengths are $\alpha = 0.18$ and $\beta = 0.08$, the ODE system (1.2) is also asymptotically stable at equilibrium (u_*, v_*, u_*, v_*).

(2) Assuming that there exists diffusion term in the system, and $\alpha = \beta = 0$, we can obtain that the PDE system (1.1) is still asymptotically stable at positive equilibrium (u_*, v_*). However, if the coupling strengths are $\alpha = 0.18$ and $\beta = 0.08$, the PDE system (1.2) begin to appear Turing instability at equilibrium (u_*, v_*, u_*, v_*).

In the following, we will display that numerical results are consistent with the theoretical results when $\sigma = 0.14$, $\alpha = 0.18$, $\beta = 0.08$, $m_1 = 10$, $n_1 = 0$. The initial values are $u01 = 0.00002\cos(5\pi x) + 0.00032\cos(5\pi y)$, $v01 = 0.09\cos(5\pi y) + 0.0004\cos(5\pi x)$, $u02 = 0.0004\cos(5\pi x) - 0.03\cos(5\pi y)$ and $v02 = 0.00002\cos(5\pi y) + 0.003\cos(5\pi x)$. Fig.11 shows that the stripe patterns produced by $u_1(x, y)$ do not change with the increase of time ($v_1(x, y)$ is the same). It is verified that when the coupling strengths are added, all the roots of $\Gamma_1(k_1)(\lambda) = 0$ still have negative real parts and do not change over time. Figs.12 and 13 show that, under the same initial value with Fig.11, the patterns of $u_2(x, y)$ and $v_2(x, y)$ change from stripe to spot with the increase of time, which verify that when the coupling strengths are

added, the roots of $\Gamma_2(k_1)(\lambda) = 0$ have at least one positive root. Therefore, the system (1.2) is Turing instability at equilibrium (u_*, v_*, u_*, v_*).

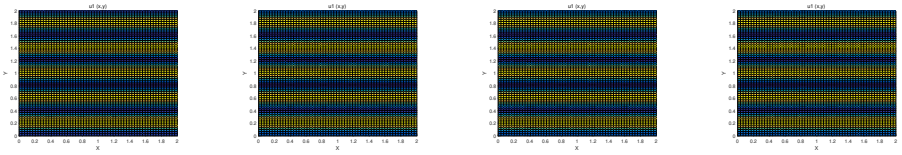

(a) $t = 560$ (b) $t = 2890$ (c) $t = 3450$ (d) $t = 4500$

Figure 11. Stripe patterns produced by $u_1(x, y)$ when $m_1 = 10$, $n_1 = 0$.

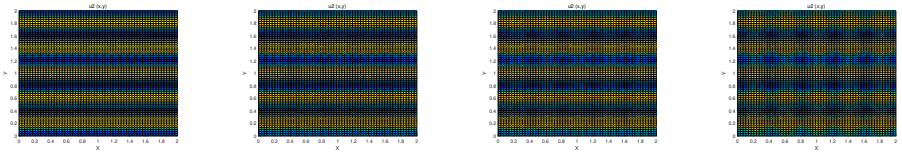

(a) $t = 560$ (b) $t = 2890$ (c) $t = 3450$ (d) $t = 4500$

Figure 12. Spot patterns produced by $u_2(x, y)$ when $m_1 = 10$, $n_1 = 0$.

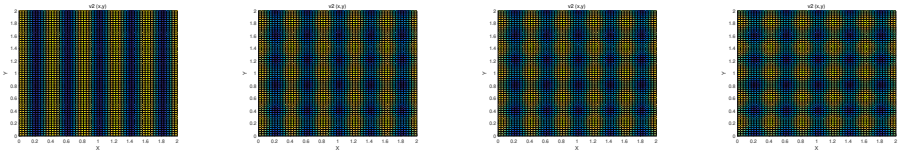

(a) $t = 560$ (b) $t = 2890$ (c) $t = 3450$ (d) $t = 4500$

Figure 13. Spot patterns produced by $v_2(x, y)$ when $m_1 = 10$, $n_1 = 0$.

When $\sigma = 0.14$, $\alpha = 0.18$, $\beta = 0.08$, $m_3 = 8$, $n_3 = 6$, by similar approach, the initial values are $u01 = 0.00002\cos(4\pi x)\cos(3\pi y) + 0.00032\cos(3\pi x)\cos(4\pi y)$, $v01 = 0.09\cos(3\pi x)\cos(4\pi y) + 0.0004\cos(4\pi x)\cos(3\pi y)$, $u02 = 0.05\cos(4\pi x)\cos(3\pi y) + 0.008\cos(3\pi x)\cos(4\pi y)$, and $v02 = 0.00002\cos(3\pi x)\cos(4\pi y) + 0.001\cos(4\pi x)\cos(3\pi y)$. Fig.14 shows that the rectangular patterns produced by $u_1(x, y)$ do not change with the increase of time ($v_1(x, y)$ is the same). Figs.15 and 16 show that, under the same initial value with Fig.14, the patterns of $u_2(x, y)$ and $v_2(x, y)$ change from rectangular to square with the increase of time.

4. Conclusions

The coupled and uncoupled FHN models with diffusion are important neural network models. The properties of Turing bifurcation and Turing instability of these models are closely related to diffusion and coupling strengths.

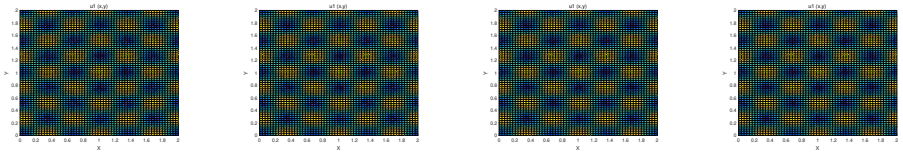

(a) $t = 390$ (b) $t = 1670$ (c) $t = 3060$ (d) $t = 4280$

Figure 14. Rectangular patterns produced by $u_1(x, y)$ when $m_3 = 8$, $n_3 = 6$.

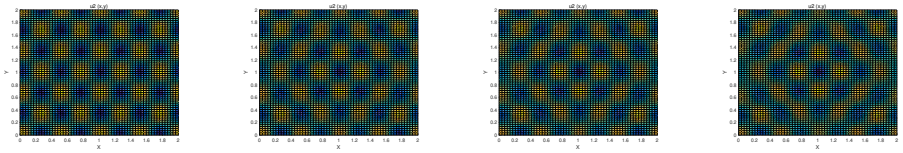

(a) $t = 390$ (b) $t = 1670$ (c) $t = 3060$ (d) $t = 4280$

Figure 15. Square patterns produced by $u_2(x, y)$ when $m_3 = 8$, $n_3 = 6$.

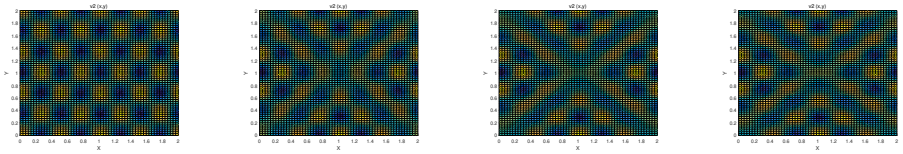

(a) $t = 390$ (b) $t = 1670$ (c) $t = 3060$ (d) $t = 4280$

Figure 16. Square patterns produced by $v_2(x, y)$ when $m_3 = 8$, $n_3 = 6$.

Firstly, the conditions for Turing bifurcation and Turing instability of the FHN model are given in Theorem 2.1. The eigenvalues of $-\Delta$ can be single, double, or higher multiplicity respectively. Hence, the state bifurcation will be single, double, three-fold, four-fold, and so on. Patterns are given which correspond to the multiplicity of state bifurcation in numerical simulations: (1) stripe and rectangular patterns correspond to simple bifurcation; (2) spot and square patterns correspond to double bifurcation; (3) highly developed square pattern correspond to four-fold bifurcation. Then, according to Theorem 3.1, by selecting appropriate values of coupling strengths α and β, Turing instability occurs in the coupled FHN model. Theoretical analysis shows that under the hypothesis of Theorem 3.1, the coupling strengths affect the stability of the system (1.2) only when there exits diffusion. Furthermore, numerical simulations present that the patterns of the coupled FHN model change from the stripe (rectangular) to spot (square) with the increase of time.

Acknowledgements

The authors are very grateful to the reviewers and the editors for their valuable suggestions and comments on improving the presentation of this paper.

References

[1] I. Biktasheva, A. Holden and V. Biktashev, *Localization of response functions of spiral waves in the FitzHugh-Nagumo system*, Int. J. Bifurcation Chaos, 2006, 16(5), 1547–1555.

[2] N. Buric and D. Todorovic, *Dynamics of FitzHugh-Nagumo excitable systems with delayed coupling*, Phys. Rev. E, 2003, 67(2), 066222.

[3] S. Chowdhury, M. Biswas and R. Dutta, *Approximate controllability of the FitzHugh-Nagumo equation in one dimension*, J. Differ. Equ., 2020, 268(7), 3497–3563.

[4] B. Ermentrout, *Stripes or spots? Nonlinear effects in bifurcation of reaction-diffusion equations on the square*, Proc. R. Soc. A-Math. Phys. Eng. Sci., 1991, 434(1891), 413–417.

[5] G. Ermentrout and J. Cowan, *A mathematical theory of visual hallucination patterns*, Biol. Cybern., 1979, 34(3), 137–150.

[6] P. Fife, *Mathematical aspects of reacting and diffusing systems*, Springer-Verlag, 1979.

[7] R. Fitzhugh, *Impulses and physiological states in theoretical models of nerve membrane*, Biophys. J., 1961, 1(6), 445–466.

[8] D. Fan and L. Hong, *Hopf bifurcation analysis in a synaptically coupled FHN neuron model with delays*, Commun. Nonlinear Sci. Numer. Simul., 2010, 15(7), 1873–1886.

[9] P. Gong and J. Xu, *Global dynamics and stochastic resonance of the forced FitzHugh-Nagumo neuron model*, Phys. Rev. E, 2001, 63(3), 031906.

[10] V. Gaiko, *Global bifurcations of multiple limit cycles in the FitzHugh-Nagumo system*, Mathematics, 2011, 74(18), 7532–7542.

[11] A. Hodgkin and A. Huxley, *A quantitative description of membrane current and its application to conduction and excitation in nerve*, J. Physiol. London, 1952, 117(4), 500–544.

[12] W. Jiang, H. Wang and X. Cao, *Turing instability and Turing-Hopf bifurcation in diffusive Schnakenberg systems with gene expression time delay*, J. Dyn. Differ. Equ., 2018, 31(4), 2223–2247.

[13] A. Jalnine, *Hyperbolic and non-hyperbolic chaos in a pair of coupled alternately excited FitzHugh-Nagumo systems.* Commun. Nonlinear Sci. Numer. Simul., 2013, 23(1–3), 202–208.

[14] G. Le, A. Pocheau and V. Croquette, *Square versus roll pattern at convective threshold*, Phys. Rev. Lett., 1985, 54(23), 2501–2504.

[15] J. Li, H. Wang and Q. Ouyang, *Square Turing patterns in reaction-diffusion systems with coupled layers*, Chaos, 2014, 24(2), 023115.

[16] J. Murray, *Mathematical biology*, Biomath, 2002, 19(1–2), 261–283.

[17] S. Mohyud-Din, Y. Khan, N. Faraz, et al., *Exp-function method for solitary and periodic solutions of Fitzhugh-Nagumo equation*, Int. J. Numer. Methods Heat Fluid Flow, 2012, 22(3), 335–341.

[18] Y. Nishiura, *Global structure of bifurcating solutions of some reaction-diffusion system*, SIAM Journal on Mathematical Analysis, 1982, 13(4), 555–593.

[19] J. Nagumo, S. Arimoto and S. Yoshizawa, *An active pulse transmission line simulating nerve axon*, Proceedings of the Ire, 1962, 50(10), 2061–2070.

[20] I. Nagy, V. Romanovski and J. Toth, *Two nested limit cycles in two-species reactions*, Mathematics, 2020, 8(10), 1658.

[21] Q. Ouyang, *Nonlinear science and pattern dynamics*, Peking University Press, Beijing, 2010.

[22] D. Olmos and B. Shizgal, *Pseudospectral method of solution of the Fitzhugh-Nagumo equation*, Math. Comput. Simul., 2009, 79(7), 2258–2278.

[23] M. Pierre, T. Suzuki and H. Umakoshi, *Asymptotic behavior in chemical reaction-diffusion systems with boundary equilibria*, J. Appl. Anal. Comput., 2018, 8(3), 836–858.

[24] R. Rameh, E. Cherry and R. Santos, *Single-variable delay-differential equation approximations of the Fitzhugh-Nagumo and Hodgkin-Huxley models*, Commun. Nonlinear Sci. Numer. Simul., 2020, 82, 105066.

[25] B. Sounvoravong and S. Guo, *N-dark soliton solutions for the multicomponen Maccari system*, Journal of Nonlinear Modeling and Analysis, 2019, 1(3), 319–334.

[26] Y. Song, H. Jiang and Y. Yuan, *Turing-Hopf bifurcation in the reaction-diffusion system with delay and application to a diffusive predator-prey model*, J. Appl. Anal. Comput., 2019, 9(3), 1132–1164.

[27] Y. Song, S. Wu and H. Wang, *Spatiotemporal dynamics in the single population model with memory-based diffusion and nonlocal effect*, J. Differ. Equ., 2019, 267(11), 6316–6251.

[28] Y. Song and J. Xu, *Inphase and antiphase synchronization in a delay-coupled system with applications to a delay-coupled FitzHugh-Nagumo system*, IEEE Trans. Neural Netw. Learn. Syst., 2012, 23(10), 1659–1670.

[29] A. Turing, *The chemical basis of morphogenesis. Philosophical Transactions of The Royal Society, Series B*, Biological Sciences, 1952, 237(641), 37–72.

[30] C. Varea, J. Aragon and R. Barrio, *Confined Turing patterns in growing systems*, Phys. Rev. E, 1997, 56(1), 1250–1253.

[31] C. Wagner, H. Muller and K. Knorr, *Pattern formation at the bicritical point of the Faraday instability*, Phys. Rev. E, 2003, 68(6), 066204.

[32] C. Zhang, A. Ke and B. Zheng, *Patterns of interaction of coupled reaction-diffusion systems of the FitzHugh-Nagumo type*, Nonlinear Dyn., 2019, 97(2), 1451–1476.